Complex role of STIM1 in the activation of store-independent Orai1/3 channels

Xuexin Zhang,[1] Wei Zhang,[1] José C. González-Cobos,[1] Isaac Jardin,[2] Christoph Romanin,[2] Khalid Matrougui,[3] and Mohamed Trebak[1]

[1]Nanobioscience Constellation, State University of New York College of Nanoscale Science and Engineering, Albany, NY 12203
[2]Institute of Biophysics, Johannes Kepler University Linz, 4020 Linz, Austria
[3]Department of Physiology, Eastern Virginia School of Medicine, Norfolk, VA 23501

Orai proteins contribute to Ca^{2+} entry into cells through both store-dependent, Ca^{2+} release–activated Ca^{2+} (CRAC) channels (Orai1) and store-independent, arachidonic acid (AA)-regulated Ca^{2+} (ARC) and leukotriene C_4 (LTC_4)-regulated Ca^{2+} (LRC) channels (Orai1/3 heteromultimers). Although activated by fundamentally different mechanisms, CRAC channels, like ARC and LRC channels, require stromal interacting molecule 1 (STIM1). The role of endoplasmic reticulum–resident STIM1 (ER-STIM1) in CRAC channel activation is widely accepted. Although ER-STIM1 is necessary and sufficient for LRC channel activation in vascular smooth muscle cells (VSMCs), the minor pool of STIM1 located at the plasma membrane (PM-STIM1) is necessary for ARC channel activation in HEK293 cells. To determine whether ARC and LRC conductances are mediated by the same or different populations of STIM1, Orai1, and Orai3 proteins, we used whole-cell and perforated patch-clamp recording to compare AA- and LTC_4-activated currents in VSMCs and HEK293 cells. We found that both cell types show indistinguishable nonadditive LTC_4- and AA-activated currents that require both Orai1 and Orai3, suggesting that both conductances are mediated by the same channel. Experiments using a nonmetabolizable form of AA or an inhibitor of 5-lipooxygenase suggested that ARC and LRC currents in both cell types could be activated by either LTC_4 or AA, with LTC_4 being more potent. Although PM-STIM1 was required for current activation by LTC_4 and AA under whole-cell patch-clamp recordings in both cell types, ER-STIM1 was sufficient with perforated patch recordings. These results demonstrate that ARC and LRC currents are mediated by the same cellular populations of STIM1, Orai1, and Orai3, and suggest a complex role for both ER-STIM1 and PM-STIM1 in regulating these store-independent Orai1/3 channels.

The Journal of General Physiology

INTRODUCTION

The universal second messenger Ca^{2+} controls numerous physiological and pathophysiological cell processes (Clapham, 2007; Cahalan and Chandy, 2009; Hogan et al., 2010). Orai channels contribute Ca^{2+} entry pathways through either store-dependent, Ca^{2+} release–activated Ca^{2+} (CRAC) channels (encoded by Orai1) (Putney, 1990; Hoth and Penner, 1992; Feske et al., 2006; Vig et al., 2006; Zhang et al., 2006), or store-independent, arachidonic acid (AA)-regulated Ca^{2+} (ARC; Mignen and Shuttleworth, 2000; Mignen et al., 2008) and leukotriene C_4 (LTC_4)-regulated Ca^{2+} (LRC; González-Cobos et al., 2013; Zhang et al., 2013) channels (encoded by both Orai1 and Orai3). Over the past two decades, Ca^{2+} entry through CRAC channels has become appreciated as a ubiquitous receptor-regulated, PLC-dependent Ca^{2+} entry pathway that controls various physiological functions in different cellular systems (Cahalan et al., 2007; Hogan and Rao, 2007; Lewis, 2011; Courjaret and Machaca, 2012; Feske et al., 2012; Trebak, 2012; Lompre et al., 2013; Srikanth and Gwack, 2013). The mechanisms of activation of store-dependent CRAC channels have been intensely studied over the past 7 years and are therefore relatively well understood (Lewis, 2011; Derler et al., 2012; Srikanth and Gwack, 2012; Prakriya, 2013). Receptor-mediated activation of PLC hydrolyzes phosphatidylinositol 4,5-bisphopshate into diacylglycerol and inositol 1,4,5-trisphosphate. The latter binds to 1,4,5-trisphosphate receptors on the ER, leading to Ca^{2+} release and store depletion (Berridge, 1993). The depletion of ER Ca^{2+} is sensed by the ER Ca^{2+} sensor, stromal

W. Zhang and J.C. González-Cobos contributed equally to this paper. Correspondence to Xuexin Zhang: xzhang21@albany.edu; or Mohamed Trebak: mtrebak@albany.edu

José C. González-Cobos's present address is Barlovento Brewing Company, Manatí 00674, Puerto Rico.

Abbreviations used in this paper: 2-APB, 2-aminoethoxydiphenyl borate; 5-LO, 5-lipooxygenase; AA, arachidonic acid; ARC, AA-regulated Ca^{2+}; CAD, Ca^{2+} release–activated Ca^{2+}–activating domain; CRAC, Ca^{2+} release–activated Ca^{2+}; DVF, divalent free; ETYA, eicosatetraynoic acid; LRC, leukotriene C_4–regulated Ca^{2+}; LTC_4, leukotriene C_4; LTC_4S, LTC_4 synthase; NDGA, nordihydroguaiaretic acid; $NMLTC_4$, *N*-methyl LTC_4; PM, plasma membrane; shRNA, short hairpin RNA; siRNA, small interference RNA; SOAR, stromal interacting molecule/Orai-activating region; STIM1, stromal interacting molecule 1; VSMC, vascular smooth muscle cell.

The Rockefeller University Press $30.00
J. Gen. Physiol. Vol. 143 No. 3 345–359
www.jgp.org/cgi/doi/10.1085/jgp.201311084

interacting molecule 1 (STIM1), leading to STIM1 aggregation and its translocation to regions where the ER is close to the plasma membrane (PM; within 25 nm) (Liou et al., 2005; Roos et al., 2005) to physically interact with Orai1 channels and activate CRAC-mediated Ca^{2+} entry. A minimal 100–amino acid cytosolic C-terminal domain of STIM1 called STIM/Orai-activating region (SOAR) or CRAC-activating domain (CAD) is involved in the physical interaction with Orai1 C and N termini (Park et al., 2009; Yuan et al., 2009). ARC channels were characterized biophysically and molecularly by Shuttleworth and coworkers (Mignen et al., 2003). Shuttleworth and coworkers reported that ARC channels have a small conductance and are highly Ca^{2+} selective in a manner similar to CRAC channels (Mignen and Shuttleworth, 2000). ARC channel activation is specifically dependent on the application of exogenous and relatively low concentrations of AA (8 µM) (Mignen and Shuttleworth, 2000; Shuttleworth, 2012). ARC channels mediate a store-independent Ca^{2+} entry pathway encoded by both Orai1 and Orai3, and were proposed to be regulated by the minor pool of STIM1 located in the PM (Mignen et al., 2007, 2008). A recent study by the same group described basal interactions between a PM-targeted C-terminal domain of STIM1 and Orai3, which are necessary for ARC channel activation (Thompson and Shuttleworth, 2013). More recent work from our laboratory in primary vascular smooth muscle cells (VSMCs) has defined LRC channels as store-independent Ca^{2+}-selective channels activated physiologically by the agonist thrombin through production and cytosolic action of LTC_4 (González-Cobos et al., 2013). LRC channels share many ARC-like features, including dependence on Orai1, Orai3, and STIM1; store independence; and requirement for basal Orai3/STIM1 precoupling (González-Cobos et al., 2013; Zhang et al., 2013). However, we revealed some unexpected differences between ARC channels as described in HEK293 cells and LRC channels in VSMCs, namely: (a) requirement of AA metabolism into LTC_4 through the actions of 5-lipooxygenase (5-LO) and LTC_4 synthase (LTC_4S) for LRC channel activation by thrombin (González-Cobos et al., 2013; Zhang et al., 2013); and (b) unlike ARC channels in HEK293 cells, ER-STIM1 is required and sufficient for LRC channel activation by agonist in VSMCs, as determined with Fura2 imaging (Zhang et al., 2013). In light of the striking similarities between ARC and LRC pathways, the two aforementioned differences between these two conductances prompted us to determine whether ARC and LRC conductances are mediated by the same cellular populations of STIM1/Orai1/Orai3 or whether they are encoded by different pools of STIM1/Orai1/Orai3 proteins, thus representing two distinct and specialized conductances reflecting differences between HEK293 cells and VSMCs. To address this question, we performed a thorough comparison between HEK293 cells and VSMCs. Using improved low noise–high resistance (>16 GΩ) whole-cell and nystatin perforated patch-clamp electrophysiological recordings, we amplified and measured reliably tiny highly Ca^{2+}-selective, Orai-mediated currents from VSMCs and HEK293 cells. We show that both HEK293 cells and VSMCs display indistinguishable nonadditive LTC_4- and AA-activated currents that are encoded by both Orai1 and Orai3. The use of a nonmetabolizable form of AA and an inhibitor of 5-LO in both cell types suggested promiscuity of channel activation by LTC_4 and AA, with LTC_4 being the most potent activator in both cell types, suggesting that ARC and LRC are mediated by the same channel entity. Surprisingly, although PM-STIM1 is required for current activation by LTC_4 and AA under whole-cell patch-clamp recordings in both cell types, ER-STIM1 is sufficient when intact cells are considered, suggesting a complex requirement for both ER-STIM1 and PM-STIM1 in regulating these store-independent Orai1/3 channels.

MATERIALS AND METHODS

Reagents

AA, Cs-methanesulfonate, Na-methanesulfonate, and nordihydroguaiaretic acid (NDGA) were purchased from Sigma-Aldrich. LTC_4, *N*-methyl LTC_4 ($NMLTC_4$), and eicosatetraynoic acid (ETYA) were from Cayman. 2-Aminoethoxydiphenyl borate (2-APB) was purchased from EMD Millipore. Cs-1,2-bis-(2-aminophenoxy) ethane-*N*,*N*,*N*′,*N*′-tetraacetic acid (Cs-BAPTA) was purchased from Invitrogen. $GdCl_3$ was from Acros Organics. All small interference RNAs (siRNAs) were purchased from Dharmacon and have been described previously (Abdullaev et al., 2008; González-Cobos et al., 2013; Motiani et al., 2013; Shinde et al., 2013; see also Table S1). The transfection kits (VCA-1003 for HEK293 cells and VPI-1004 for VSMCs) were from Lonza. All other chemicals were from Thermo Fisher Scientific.

VSMC isolation and cell culture

HEK293 cells (ATCC) were cultured in a 75-CM^2 flask. Before patch-clamp recordings, we seeded cells on glass coverslips. Cells were cultured in Dulbecco's modified Eagle's medium (DMEM) with 1% L-glutamine, 1% sodium pyruvate (Corning), 10% fetal bovine serum (FBS; HyClone Laboratories, Inc.), and 1% antibiotic-antimycotic (Invitrogen). Cells were cultured at 37°C in 5% CO_2-air atmosphere.

The use of rats for these experiments has been reviewed and approved by the Institutional Animal Care and Use Committee at State University of New York Albany Animal Resource Facility, which is licensed by the US Department of Agriculture and the Division of Laboratories and Research of the New York State Department of Public Health. For VSMC isolation, male adult rats (250–300 g) were euthanized, and aortas were dissected out into ice-cold physiological saline solution. Fat tissues and endothelium were removed completely. The artery was cut into small pieces and digested with a papain solution for 20 min at 37°C, and then with a mixture of collagenase II and collagenase H for 15 min at 37°C. The digestion solution was removed, and the cells were washed and gently liberated with a fire-polished glass pipette and transferred to culture plates. Isolated VSMCs were maintained in culture (45% DMEM and 45% Ham's F-12 supplemented with 10% FBS, 1% L-glutamine, and 1% antibiotic-antimycotic) at 37°C, 5% CO_2, and 100% humidity, passaged, and used within four to eight passages in all experiments.

Cell transfections

All transfections in VSMCs were done using the Nucleofector device II (Amaxa Biosystems) and program D-033 according to the manufacturer's instructions. Green fluorescent protein was either cotransfected with siRNA or encoded by the short hairpin RNA (shRNA) vectors for identification of successfully transfected cells. All transfections in HEK293 cells were done using program Q-001 with Nucleofector device II.

Electrophysiology

Whole-cell and nystatin perforated patch-clamp electrophysiological recordings were performed using an Axopatch 200B and Digidata 1440A (Molecular Devices) as described previously (Zhang et al., 2011; González-Cobos et al., 2013). Pipettes were pulled from borosilicate glass capillaries (World Precision Instruments, Inc.) with a flaming/brown micropipette puller (P-97; Sutter Instrument) and polished using DMF1000 (World Precision Instruments, Inc.). Resistances of filled pipettes were 2–3 MΩ. The liquid-junction potential offset caused by different internal and external saline composition was −4.7 mV and was corrected. Series resistances were <10 MΩ. Immediately before the experiments, cells were washed with bath solution. Only cells with tight seals (>16 GΩ) were selected for break in. Cells were maintained at a 0-mV holding potential during experiments and subjected to voltage ramps from +100 to −140 mV lasting 250 ms every 2 s. Immediately after establishing the whole-cell configuration, a first 30-s divalent-free (DVF) pulse (before current development in response to LTC_4 dialysis or before application of exogenous AA) is applied to gauge maximal background current. The I-V curves obtained in DVF bath solutions representing the maximal background current are averaged and then subtracted from the average I-V of LTC_4- or AA-activated Na^+ currents obtained in DVF bath solutions when the current is maximally activated by the stimulus. These subtracted I-V curves are represented as independent I-V curves in all figures. Data represented in Tables 1 and S1 represent inward currents taken at −100 mV. These values were obtained by averaging background currents for all the ramps during the first DVF pulse and subtracting them from the corresponding average currents for the second DVF pulse when stimuli-activated currents are maximal. "Reverse" ramps were designed to inhibit Na^+ channels potentially expressed in VSMCs. 8 mM $MgCl_2$ was included in the pipette solution to inhibit TRPM7 currents. Clampfit 10.1 software (Molecular Devices) was used for data analysis.

Solutions for electrophysiological recordings

DVF solution contained: 155 mM Na-methanesulfonate, 10 mM HEDTA, 1 mM EDTA, and 10 mM HEPES, pH 7.4, adjusted with NaOH.

AA-activated currents

Bath solution contained: 115 mM Na-methanesulfonate, 10 mM CsCl, 1.2 mM $MgSO_4$, 10 mM HEPES, 20 mM $CaCl_2$, and 10 mM glucose with pH adjusted to 7.4 with NaOH. 8 µM AA was added to the bath where indicated in the figures. Pipette solution contained: 115 mM Cs-methanesulfonate, 10 mM Cs-BAPTA, 5 mM $CaCl_2$, 8 mM $MgCl_2$, and 10 mM HEPES, with pH adjusted to 7.2 with CsOH. Calculated free Ca^{2+} was 150 nM using Maxchelator software.

LTC_4-activated currents

Bath solution contained: 115 mM Na-methanesulfonate, 10 mM CsCl, 1.2 mM $MgSO_4$, 10 mM HEPES, 20 mM $CaCl_2$, and 10 mM glucose, with pH adjusted to 7.4 with NaOH. Pipette solution contained: 115 mM Cs-methanesulfonate, 10 mM Cs-BAPTA, 5 mM $CaCl_2$, 8 mM $MgCl_2$, and 10 mM HEPES, with pH adjusted to 7.2 with CsOH. 100 nM LTC_4 was included in the patch pipette.

Store depletion–activated currents

Bath solution contained: 115 mM Na-methanesulfonate, 10 mM CsCl, 1.2 mM $MgSO_4$, 10 mM HEPES, 20 mM $CaCl_2$, and 10 mM glucose, with pH adjusted to 7.4 with NaOH. Pipette solution contained: 115 mM Cs-methanesulfonate, 20 mM Cs-BAPTA, 8 mM $MgCl_2$, and 10 mM HEPES, with pH adjusted to 7.2 with CsOH.

Solutions for perforated patch-clamp electrophysiology

Bath solution contained: 115 mM Na-methanesulfonate, 10 mM CsCl, 1.2 mM $MgSO_4$, 10 mM HEPES, 20 mM $CaCl_2$, and 10 mM glucose, with pH adjusted to 7.4 with NaOH. Pipette solution contained: 125 mM Cs-methanesulfonate, 5 mM KCl, 1 mM $CaCl_2$, 7 mM $MgCl_2$, 10 mM HEPES, and 10 mM glucose, with pH adjusted to 7.4 with NaOH. 200 µg/ml nystatin was included in the patch pipette.

Erase and replace experiments

Cells were transfected with either nontargeting control siRNA (siControl) or siRNA targeting to STIM1 (siSTIM1) and incubated for 72 h. Cells were then detached and electroporated again with siSTIM1 along with siRNA-resistant plasmids encoding different versions of STIM1 (3 µg plasmid cDNA per 10^6 cells). Cells were allowed to recover for an additional 36 h before recording. Protein expression of STIM1 constructs was verified by Western blots and fluorescence (for eYFP-STIM1 plasmids).

Biotinylation of cell surface membrane proteins

HEK293 cells were transfected either with eYFP N-terminally tagged or untagged WT STIM1. After 24 h, cell surface proteins were biotinylated for 30 min at 4°C using sulfo-NHS-LC-LC- (0.5 mg/ml; Thermo Fisher Scientific). In brief, cells were incubated for 30 min at 4°C with the biotinylation reagent. After incubation, 100 mM Tris was added to stop the reaction. Cells were washed twice with PBS to remove excess biotinylation agent and lysed with lysis buffer, pH 8.0, containing 100 mM NaCl, 20 mM Tris, 2 mM EDTA, 10% glycerol, and 0.5% Nonidet P-40, and supplemented by 20 µl/ml protease inhibitor cocktail (Roche). Lysed samples were centrifuged at 14,000 *g* for 15 min. Finally, biotinylated proteins in the supernatant were precipitated using High Capacity Streptavidin Agarose Resin (Thermo Fisher Scientific) overnight at 4°C on a rocking platform. The samples were resolved by 10% SDS-PAGE, and protein detection was done using anti-STIM1 antibody.

Western blotting

Cultured cells were detached from dishes and centrifuged. The cell pellets were lysed using RIPA lysis buffer (50 mM Tris-HCl, pH 8.0, 150 mM NaCl, 1% Triton X-100, 0.2 mM EDTA, 0.1% SDS, 0.5% sodium deoxycholate, 2 mM PMSF, 10% protease inhibitor cocktail [Roche], and 10% phosphatase inhibitor cocktail [Roche]). Protein concentrations were determined by BCA protein assay reagent (Thermo Fisher Scientific), and the denatured proteins (10–20 µg) were boiled for 10 min in 4× sample buffer containing 20 mM DTT and subjected to SDS-PAGE (8–14%). Proteins were electrotransferred onto polyvinylidene difluoride membranes (Bio-Rad Laboratories). After the blots were blocked with 5% nonfat dry milk (NFDM) dissolved in Tris-buffered saline containing 0.1% Tween 20 (TTBS) for 2 h at room temperature, they were washed three times with TTBS for 5 min each and incubated overnight at 4°C with specific primary antibodies (anti-STIM1 [1:250 dilution; BD], anti-Orai1 [1:1,000 dilution; Alomone], or anti-Orai3 [C terminal; 1:125 dilution; ProSci]) in TTBS containing 1% BSA. On the next day, membranes were washed (three times for 5 min each) with TTBS and incubated for 1 h at room temperature with horseradish peroxidase–conjugated secondary antibodies (anti–mouse antibody [1:10,000 dilution]; Jackson ImmunoResearch Laboratories, Inc.) or anti–rabbit IgG (1:10,000 dilution; Jackson ImmunoResearch Laboratories, Inc.) in TTBS containing 2% NFDM. Protein bands were visualized by enhanced chemiluminescence using Super Signal West Pico or Femto reagents (Thermo Fisher Scientific). Signal intensity was measured with

an Imaging Station (LAS4000; Fujifilm). Membranes were then stripped and reprobed with β-actin antibody (β-actin NH2-terminal domain; 1:35,000 dilution; Sigma-Aldrich) to verify equal loading. Densitometric analysis was performed using ImageJ software.

RT-PCR and real-time PCR

Total RNA was extracted from VSMCs using the RNeasy Mini kit (QIAGEN) according to the manufacturer's protocol. cDNA was made from 0.5 µg RNA reverse transcribed using oligo (dT) primers (Invitrogen) and SuperScript III reverse transcription (Invitrogen). PCR reactions were completed using Illustra PuReTaq Ready-To-Go PCR beads (GE Healthcare). The sense and antisense primers targeting Orai isoforms are described in Table S2. All primers we used in this paper were synthesized by Integrated DNA Technologies. The PCR amplification was done using a MyCycler Thermal Cycler (Bio-Rad Laboratories). Amplification started with initial denaturation at 94°C for 5 min, and then 40 cycles of denaturation at 94°C for 30 s, annealing at 55°C for 1 min, and extension at 72°C for 2 min. Gel electrophoresis was used to identify the PCR products in a 1% agarose gel using ethidium bromide staining. Real-time PCR analysis was performed using an iCycler and iCycler iQ Optical System software (Bio-Rad Laboratories). PCR reactions were performed using iQ SYBR Green Supermix (Bio-Rad Laboratories). The PCR protocol started with 5 min at 94°C, followed by 45 cycles of 30 s at 94°C, 30 s at 54.3°C, and 45 s at 72°C. Quantification was measured as sample fluorescence crossed a predetermined threshold value that was just above the background. Expressions of Orai isoforms were compared with those of the housekeeping gene rpl32 and were measured using comparative threshold cycle values.

Statistics

For patch clamp, data are expressed as mean/range; for qRT-PCR, data are represented as mean ± SEM. Statistical analyses comparing two experimental groups were performed using two-tailed *t* test with Origin 7.5 software (OriginLab). Throughout the figures *, **, and *** indicates p-values of <0.05, 0.01, and 0.001, respectively. Differences were considered significant when $P < 0.05$. Mean/range, *n* number, and p-values are reported in Tables 1 and S3 for patch-clamp data.

Online supplemental material

An online supplement is included containing 14 figures and 3 tables. The supplemental figures contain ARC recordings under Ca^{2+}-containing bath solutions (Fig. S1) as well as show the effects of Orai2 knockdown on ARC currents (Fig. S2). The supplemental figures also contain control data representing CRAC measurements in HEK293 cells and VSMCs performed in parallel to the ARC and LRC recordings depicted in the main figures (Figs. S4, 5, 6, 9, and 10). Fig. S7 addresses whether the ETYA concentration used in the study (8 µM) is submaximal, and Figs. S13 and S14 explore the role of calmodulin in LRC channel activation. Other supplemental figures show the full Western blot membranes documenting Orai1 and Orai3 knockdown (Fig. S3) and biotinylation experiments showing the expression of different forms of STIM1 proteins on the plasma membrane (Fig. S8). Tables S1 and S2 include a list of primers and siRNA/shRNA sequences used in this study, and Table S3 contains a statistical summary of all patch-clamp data represented in the supplemental figures. The online supplemental material is available at http://www.jgp.org/cgi/content/full/jgp.201311084/DC1.

RESULTS

AA activates Ca^{2+}-selective currents mediated by Orai1 and Orai3, but not Orai2, in both VSMCs and HEK293 cells

We used whole-cell patch-clamp recordings using a pipette solution where Ca^{2+} was buffered to a physiological

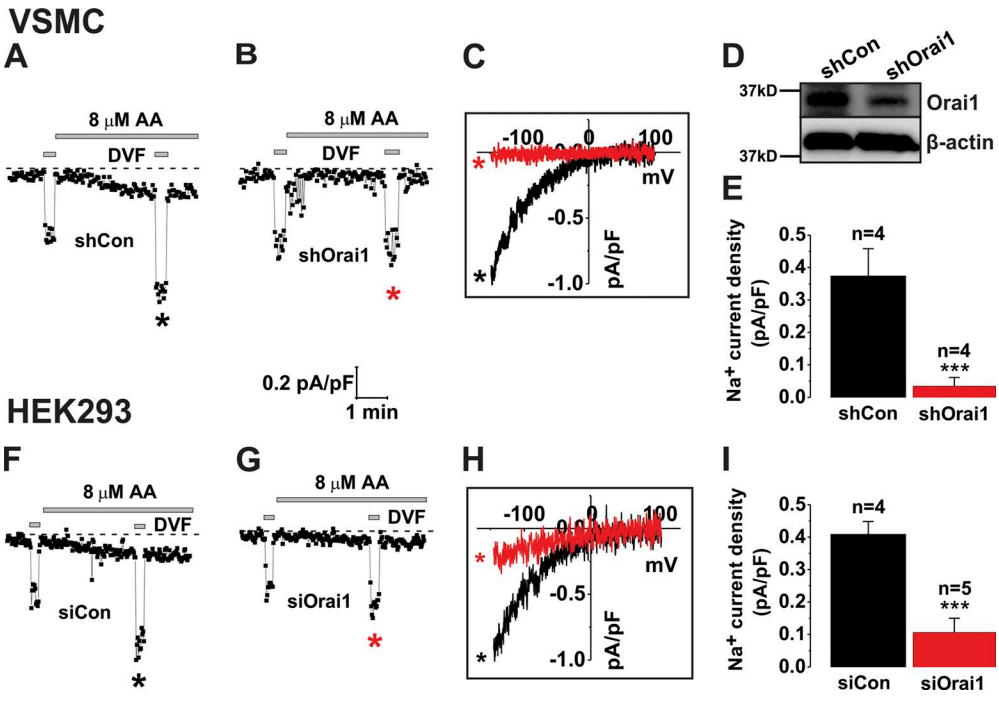

Figure 1. Orai1 is required for ARC channel activation in both VSMCs and HEK293 cells. Whole-cell electrophysiological recordings in VSMCs infected with lentiviruses encoding shRNA against Orai1 (shOrai1) or shControl, a nontargeting control. Time course of AA-activated whole-cell inward currents taken at −100 mV shows that Orai1 knockdown abrogated Na^+/Ca^{2+} ARC currents (B) as compared with control (A). In HEK293 cells, Orai1 knockdown using transfection with siRNA targeting Orai1 (siOrai1) significantly inhibited AA-activated Na^+/Ca^{2+} currents (G) as compared with control (F). Na^+ I-V relationships for AA-activated currents in VSMCs (C) and HEK293 cells (H) confirm the requirement of Orai1 for channel activation. Statistical analysis of these data is shown in E and I. Western blots performed on VSMCs shows that shRNA targeting Orai1 significantly down-regulated Orai1 protein expression (D). Values of Na^+ current densities are represented as mean/range in both VSMCs and HEK293 cells and are reported in Table 1. I-V curves in this figure and all subsequent figures and values in Table 1 were background subtracted, and values were averaged and determined as described in Materials and methods.

150 nM to show that 8 µM AA activated similar inwardly rectifying Ca^{2+}-selective currents in HEK293 cells and VSMCs. These currents were recorded in Ca^{2+}-containing (20 mM) bath solutions and amplified in DVF (Na^+ as the charge carrier) solutions (Figs. 1, A and F, and S1, A–C). These currents displayed all the key features associated with ARC channels (Mignen and Shuttleworth, 2000), including marked inward rectification, very positive (greater than +40 mV) reversal potential, resistance to inhibition by 50 µM 2-APB (Fig. S1, D–G, shows a control where CRAC Ca^{2+} currents are inhibited by 2-APB), and most critically, an activation that was specifically dependent on exogenous application of low concentrations of AA. Representative background-subtracted I-V relationships of AA-activated currents in VSMCs and HEK293 cells are shown in Fig. 1 (C and H) for Na^+ currents measured in DVF bath solutions (see also Fig. S1 B for Ca^{2+} currents in VSMCs). Statistical analysis of patch-clamp data from each figure is reported in Table 1, and details on how these values were calculated are described in Materials and methods. To determine the molecular identity of the AA-activated Ca^{2+} entry pathway, we used a molecular knockdown approach targeting all Orai isoforms in both VSMCs and HEK293 cells.

TABLE 1

Statistical analysis of patch-clamp data from figures in the main text

Figure	Cell type	Experiment	Stimulus	I[Na^+] (pA/pF) Mean/range	*n*	P-value
1 E	VSMC	shControl	AA	0.374/0.084	4	
	VSMC	shOrai1	AA	0.034/0.027	4	shOrai1 vs. shCont.; P = 2.53 E-06
1 I	HEK293	siControl	AA	0.409/0.039	4	
	HEK293	siOrai1	AA	0.106/0.044	5	siOrai vs. siCont.; P = 2.77 E-08
2 E	VSMC	Control	AA	0.389/0.117	6	
	VSMC	siOrai2	AA	0.375/0.060	4	siOrai2 vs. Cont.; P = 0.565
	VSMC	shOrai3	AA	0.051/0.069	5	shOrai3 vs. Cont.; P = 4.90 E-07
2 I	HEK293	Control	AA	0.397/0.069	4	
	HEK293	siOrai2	AA	0.380/0.096	5	siOrai2 vs. Cont.; P = 0.394
	HEK293	siOrai3	AA	0.161/0.097	5	siOrai3 vs. Cont.; P = 8.55 E-07
3 F	VSMC	WT	ETYA	0.195/0.065	6	
	VSMC	WT	AA	0.379/0.063	4	AA vs. ETYA; P = 3.59 E-06
	VSMC	WT	NDGA + AA	0.185/0.087	5	
	VSMC	WT	NDGA + LTC_4	0.384/0.066	5	NDGA+LTC_4 vs. NDGA + AA; P = 7.45 E-06
3 L	HEK293	WT	ETYA	0.191/0.053	4	
	HEK293	WT	AA	0.391/0.076	5	AA vs. ETYA; P = 1.40 E-05
	HEK293	WT	NDGA + AA	0.201/0.107	5	
	HEK293	WT	NDGA + LTC_4	0.384/0.048	5	NDGA + LTC_4 vs. NDGA + AA; P = 1.71 E-05
4 F	VSMC	WT pipette	$NMLTC_4$	0.366/0.082	4	
	VSMC	WT bath	$NMLTC_4$	0.038/0.052	5	$NMLTC_4$ in Bath vs. in pipette; P = 7.61 E-07
5 F	VSMC	siControl	AA	0.403/0.056	5	
	VSMC	siSTIM1	AA	0.039/0.102	5	siSTIM1 vs. siCont.; P = 7.57 E-08
	VSMC	+WT-STIM1	AA	0.301/0.087	6	+WT-STIM1 vs. siSTIM1; P = 3.27 E-05
	VSMC	+eYFP-STIM1	AA	0.060/0.086	4	+eYFP-STIM1 vs. siSTIM1; P = 0.436
	HEK293	siControl	AA	0.417/0.147	6	
	HEK293	siSTIM1	AA	0.037/0.056	5	siSTIM1 vs. siCont.; P = 1.51 E-07
	HEK293	+WT-STIM1	AA	0.311/0.169	5	+WT-STIM1 vs. siSTIM1; P = 1.28 E-05
	HEK293	+eYFP-STIM1	AA	0.068/0.080	5	+eYFP-STIM1 vs. siSTIM1; P = 0.158
6 F	HEK293	siControl	LTC_4	0.416/0.135	6	
	HEK293	siSTIM1	LTC_4	0.028/0.036	4	siSTIM1 vs. siCont.; P = 3.32 E-07
	HEK293	+WT-STIM1	LTC_4	0.323/0.169	5	+WT-STIM1 vs. siSTIM1; P = 8.68 E-05
	HEK293	+eYFP-STIM1	LTC_4	0.037/0.043	5	+eYFP-STIM1 vs. siSTIM1; P = 0.442
7 F	VSMC	siControl	AA	0.385/0.035	5	
	VSMC	siSTIM1	AA	0.038/0.039	5	siSTIM1 vs. siCont.; P = 3.40 E-10
	VSMC	+WT-STIM1	AA	0.315/0.149	6	+WT-STIM1 vs. siSTIM1; P = 5.84 E-07
	VSMC	+eYFP-STIM1	AA	0.331/0.126	5	+eYFP-STIM1 vs. siSTIM1; P = 4.74 E-06

Statistical analysis on patch-clamp data performed in this study organized figure by figure and showing mean/range of Na^+ currents with the corresponding *n* number and p-values. WT, wild type; AA, arachidonic acid; LTC_4, leukotriene C_4; $NMLTC_4$, *N*-methyl leukotrieneC_4; ETYA, eicosatetraynoic acid; NGDA, nordihydroguaiaretic acid.

We used infection with specific shRNA-encoding lentiviruses for VSMCs and transfection with specific siRNA sequences in HEK293 cells (see sequence in Table S1). AA-activated Ca^{2+} entry required both Orai1 and Orai3 (Figs. 1 and 2) but was independent of Orai2 in both VSMCs and HEK293 cells (Fig. S2). Knockdown of Orai1 and Orai3 proteins in VSMCs is shown in Figs. 1 D and 2 D, whereas knockdown of Orai2 is documented at the mRNA level in Fig. S2 A because of the lack of specific antibodies against Orai2. We achieved a level of knockdown of 67 ± 8% and 72 ± 4% for Orai1 and Orai3, respectively. The entire Western blots validating the specificity of Orai1 and Orai3 antibodies using knockdown and overexpression in HEK293 cells are shown in Fig. S3. Statistical analyses on Na^+ currents are shown in Figs. 1 (E and I) and 2 (E and I). Representative background-subtracted I-V curves are shown in Figs. 1 (C and H), 2 (C and H), and S2 (D and G), respectively; the first DVF pulse in all traces is applied before the addition of AA or shortly after break-in (for the case of BAPTA and LTC_4) to gauge background currents. Please note that statistics on data from each figure, including mean/range (instead of mean ± SEM) and p-values for comparisons are listed in Table 1. Store depletion–activated CRAC currents using 20-mM BAPTA dialysis through the patch pipette were used throughout as additional controls, further confirming the dependence of CRAC on Orai1 but not on Orai2 and Orai3 in both VSMCs and HEK293 cells (see Fig. S4 for Orai1 knockdown, Fig. S5 for Orai2 knockdown, and Fig. S6 for Orai3 knockdown). Note that CRAC currents show typical depotentiation in DVF solutions (Prakriya and Lewis, 2002), whereas AA-activated currents do not.

Activation of membrane currents by AA in HEK293 and VSMCs is mediated by its downstream metabolite, LTC_4

Previous studies from our group showed that thrombin activates a store-independent Ca^{2+} entry through intracrine LTC_4 originating from AA downstream metabolism by the actions of 5-LO and LTC_4S in VSMCs (González-Cobos et al., 2013). However, an earlier pharmacological study concluded that ARC channel activation is mediated

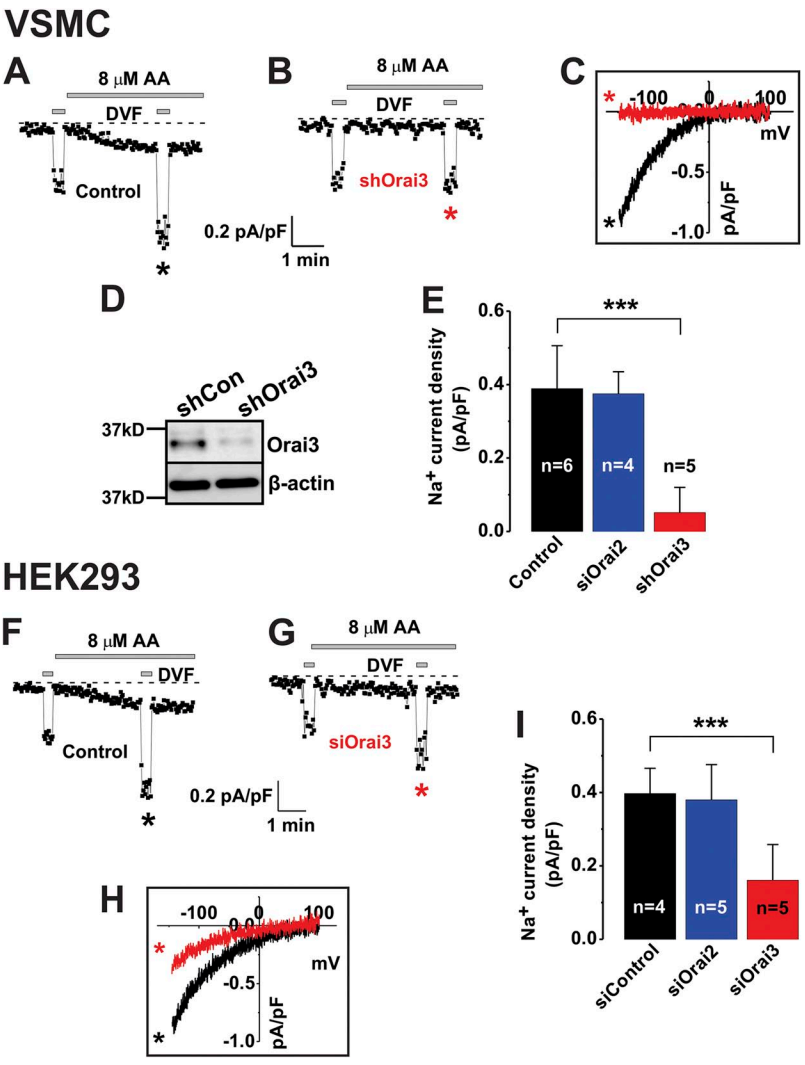

Figure 2. Orai3, but not Orai2, is uniquely required for ARC channel activation in both VSMCs and HEK293 cells. Whole-cell electrophysiological recordings in VSMCs infected with lentiviruses encoding shRNA against Orai3 (shOrai3) or shControl, a nontargeting shRNA control. Orai3 knockdown abrogated AA-activated Na^+/Ca^{2+} currents (B) as compared with control (A). In HEK293 cells, Orai3 knockdown using transfection of siRNA targeting Orai3 (siOrai3) significantly inhibited AA-activated Na^+/Ca^{2+} currents (G) as compared with control (F). Na^+ I-V relationships for AA-activated currents in VSMCs (C) and HEK293 cells (H) confirm the requirement of Orai3 for current activation. Statistical analysis of these data is shown in E and I. Effect of Orai2 knockdown with siRNA on AA-activated currents is also included in E and I; raw traces and I-V curves of Orai2 knockdown are shown in Fig. S2. Western blots performed on VSMCs shows that shOrai3 significantly down-regulated Orai3 protein expression (D). AA-activated Na^+ current densities are represented as mean/range for both VSMCs and HEK293 cells and are reported in Table 1.

by AA produced through phospholipase A2 activity and does not depend on AA metabolites (Shuttleworth, 1996). Therefore, to determine if this represents a difference between different cell types (namely, HEK293 cells and VSMCs), we sought to determine side by side in both cell types whether AA metabolism is required for current activation by AA. We tested a nonmetabolized analogue of AA (ETYA) and showed that ETYA activated a Ca^{2+}-selective current in both HEK293 cells and VSMCs, but this current was ∼50% the size of AA-activated current in both VSMCs (Fig. 3, A and B) and HEK293 cells (Fig. 3, G and H). With the use of a 5-LO inhibitor, NDGA inhibited AA-activated currents by ∼50% in both VSMCs (Fig. 3 C) and HEK293 cells (Fig. 3 I). However, NDGA had no effect on LTC_4-activated currents in both cell types (Fig. 3, D and J). Representative I-V curves are shown in Fig. 3 (E and K, respectively), and statistical analyses on Na^+ currents are shown in Fig. 3 (F and L). To rule out that the lesser effect of 8 µM ETYA on current activation is because this concentration is submaximal, we performed additional recordings in the presence of higher concentrations of ETYA. As shown in Fig. S7, increasing concentration of ETYA (up to 40 µM) failed to cause further increase in the current density.

In a different set of experiments in VSMCs, we showed that exogenous AA does not further enhance currents activated by intracellular dialysis of LTC_4 (Fig. 4, A and B), suggesting that both molecules act on the same channel entity. We also sought to determine whether LTC_4 metabolism is required for current activation, and thus we used a nonmetabolizable form of LTC_4, $NMLTC_4$. $NMLTC_4$ activated membrane currents undistinguishable from those activated by LTC_4 and AA in terms of size, biophysical properties, and pharmacology (e.g., lack of inhibition by 50 µM 2-APB; Fig. 4 C). Furthermore, $NMLTC_4$ applied in the bath solution failed to activate any currents, ruling out an action on PM cysteinyl-leukotriene receptors (Fig. 4, D–F).

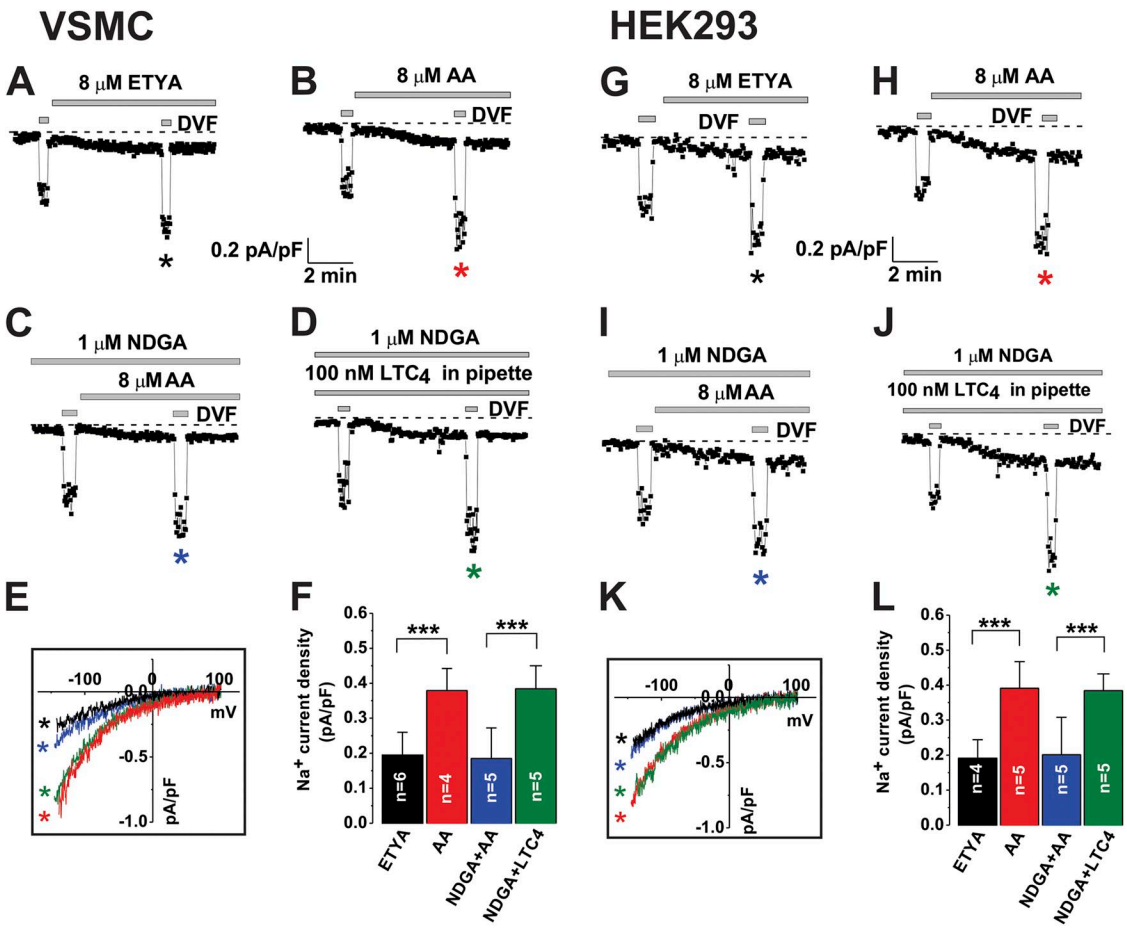

Figure 3. AA-activated currents are mediated by LTC_4 in both VSMCs and HEK293 cells. Whole-cell electrophysiological recordings in VSMCs and HEK293 cells show that ETYA, an AA-nonmetabolized analogue of activated currents (A, VSMCs; G, HEK293 cells) that were significantly smaller than AA-activated currents (B, VSMCs; H, HEK293 cells). The 5-LO inhibitor, NDGA, significantly inhibited AA-activated currents (C, VSMCs; I, HEK293 cells) but had no effect on LRC currents activated by LTC_4 dialysis through the patch pipette (D, VSMCs; J, HEK293 cells). Representative I-V curves were taken where indicated by the color-coded asterisks and are shown in E and K. Statistical analysis on current densities in VSMCs and HEK293 cells is reported as mean/range in F and L, respectively.

PM-STIM1 is required for AA-activated currents in both VSMCs and HEK293 cells under whole-cell patch-clamp conditions

We sought to confirm, using erase and replace, whether under whole-cell patch-clamp electrophysiology conditions, only the full-length untagged STIM1 capable of locating to the PM (PM-STIM1), can rescue membrane currents activated by AA in both HEK293 cells and VSMCs depleted of STIM1. Knockdown of endogenous STIM1 was achieved using specific siRNA followed by subsequent rescue with different versions of siRNA-resistant STIM1, WT untagged STIM1 (WT-STIM1) that expresses at both the ER and PM, and eYFP-tagged STIM1 that does not traffic to the PM and expresses exclusively in the ER. The inability of eYFP-STIM1 to reach the PM has been documented (Mercer et al., 2006; Hauser and Tsien, 2007). Nevertheless, we performed surface biotinylation experiments in HEK293 cells using the constructs and protocols described herein to show that only untagged STIM1 is expressed at the PM (~30% of total STIM1), whereas eYFP-STIM1 is not present on the cell surface (Fig. S8); we also show that store depletion with 2 µM thapsigargin does not affect the surface expression of either STIM1 constructs (Fig. S8). Under this protocol, where we biotinylate and then immunoprecipitate with streptavidin followed by detection with anti-STIM1 antibody using Western blot, it is possible that untagged STIM1 detected in Western blot is in fact intracellular. Such possibility would involve another PM protein associated with intracellular STIM1 (e.g., Orai1 or Orai3), which would be biotinylated and immunoprecipitated with streptavidin under our experimental conditions. The immunoprecipitation of this PM protein would pull down the intracellular STIM1 associated with it, which would be subsequently detected by anti-STIM1 antibody. However, this possibility is highly unlikely for the following reasons: (a) in cells expressing eYFP-STIM1 assayed using the same protocol, expression of eYFP-STIM1 at the PM was not detected; and (b) store depletion with thapsigargin, which causes direct STIM1/Orai associations, does not cause any change in PM expression of either untagged STIM1 or eYFP-STIM1. As expected, only WT-STIM1 rescued AA-activated currents in VSMCs (Fig. 5 C), whereas eYFP-STIM1 did not (Fig. 5 D). Ionomycin was added at the end of recordings to confirm that under both rescue conditions, CRAC currents are rescued (Fig. 5, C and D). Representative I-V curves are shown in Fig. 5 E, and statistical analyses on Na^+ currents are shown in Fig. 5 F. As a control, we also show that siRNA against STIM1 (siSTIM1) is effective at knocking down STIM1 proteins and abrogating CRAC currents activated by store depletion with 20 mM BAPTA as compared with control siRNA (siControl; Fig. S9). We further determined the amplitude of

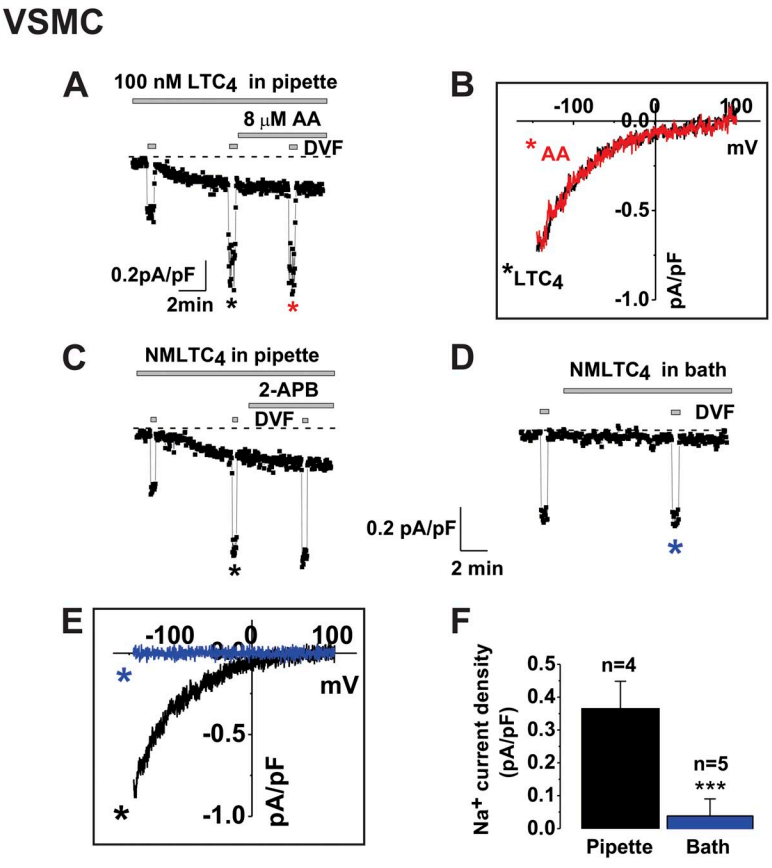

Figure 4. Nonmetabolizable LTC_4 ($NMLTC_4$) activated currents similar to those activated by LTC_4 in VSMCs. (A) Whole-cell electrophysiological recordings in VSMCs show no additivity between currents activated by inclusion of LTC_4 in the patch pipette and subsequent addition of AA to the bath solution (Na^+ I-V relationships are shown in B). (C) $NMLTC_4$, a synthetic analogue of LTC_4 that is not readily metabolized to LTD_4, and LTE_4 activated currents similar to those activated by LTC_4 and AA that were not inhibited by 50 µM 2-APB. (D) $NMLTC_4$ did not activate any currents when added to the bath solution. Representative Na^+ I-V relationships of $NMLTC_4$ data are shown in E. Statistical analysis on Na^+ current densities activated by $NMLTC_4$ is shown in F.

CRAC currents recorded from VSMCs in Ca^{2+}-containing bath solutions using the erase and replace protocol under the four conditions of transfection (siControl, siSTIM1, siSTIM1 + WT-STIM1, and siSTIM1 + eYFP-STIM1; Fig. S10). As expected and unlike AA-activated currents, CRAC currents are rescued by both versions of STIM1, WT-STIM1, and eYFP-STIM1, thus ruling out any potential artifact resulting from the expression of eYFP-STIM1. Most significantly, similar experiments performed using the same reagents, protocols, and conditions described above were performed in HEK293 cells with identical results: although CRAC currents were rescued by both versions of STIM1 (Fig. S12), only full-length untagged STIM1 capable of trafficking to the PM could rescue AA-activated currents (Fig. S11).

One important observation arising from these sets of experiments is although AA-activated current densities are rescued to near endogenous levels with ectopically expressed STIM1 (Na^+ currents of ~0.4 pA/pF at −100 mV), CRAC current densities under STIM1 rescue conditions are severalfold higher (Ca^{2+} currents of ~1 pA/pF and Na^+ currents of ~5 pA/pF at −100 mV) than endogenous CRAC (see Figs. S10 and S12).

PM-STIM1 is required for LTC_4-activated currents in HEK293 cells under whole-cell patch-clamp conditions

We have demonstrated previously that LTC_4 activated an inward Ca^{2+} current in primary VSMCs, contributed by both Orai1 and Orai3 (González-Cobos et al., 2013). Therefore, we sought to determine (a) whether LTC_4 can also activate a similar current in HEK293 cells, and (b) the pool of STIM1 required for LTC_4-regulated current activation. Intracellular dialysis of LTC_4 activated an inward Ca^{2+} current in HEK293 cells (Fig. 6 A). The size and biophysical properties of this current are similar to LRC currents recorded in VSMCs and to AA-activated ARC currents recoded from VSMCs and HEK293 cells. On knockdown of STIM1, this current was essentially eliminated (Fig. 6 B). Expression of WT-STIM1 into STIM1-depleted cells rescued LTC_4-activated current (Fig. 6 D), whereas eYFP-STIM1 expression did not (Fig. 6 E), consistent with previous studies on ARC channels in HEK293 cells and with the VSMC results described above. Representative I-V curves for all conditions are shown in Fig. 6 C, and statistical analyses on the extent of Na^+ current are shown in Fig. 6 F. In summary, our results thus far suggest that in both VSMCs and HEK293 cells, the signal

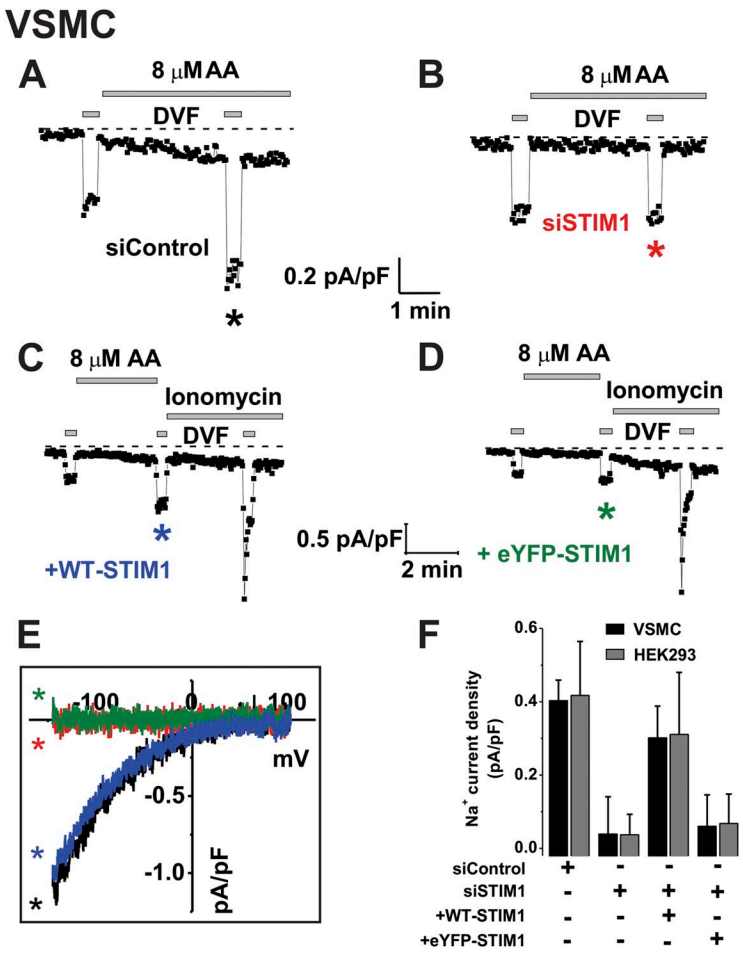

Figure 5. WT-STIM1 is required for AA-activated currents in both VSMCs and HEK293 cells. Whole-cell electrophysiological recordings in VSMCs transfected with siRNA against STIM1 (siSTIM1) or siControl, a nontargeting control. STIM1 knockdown abrogated AA-activated Na^+/Ca^{2+} currents (B) as compared with control (A). Upon ectopic expression of plasmids encoding either WT-STIM1 (C) or eYFP-STIM1 (D) after STIM1 knockdown in VSMCs, only WT-STIM1 rescued AA-activated currents (C and D). At the end of experiments depicted in C and D, CRAC currents were activated with subsequent addition of 250 nM ionomycin, thus confirming that ER-STIM1 protein was expressed and functional. Representative I-V curves were taken where indicated by the color-coded asterisks and are shown in E. Statistical analysis on current density data for all four conditions is shown in F as mean/range for both VSMCs and HEK293 cells (raw data and I-V curves for HEK293 cells are shown in Fig. S11). Please note that the scale for C and D is 2.5-fold bigger than the scale for A and B.

for the activation of store-independent Orai1/3 channels is intracrine LTC_4 originating from AA metabolism.

ER-STIM1 is sufficient to support AA-activated currents in VSMCs under nystatin perforated patch-clamp conditions

Previous studies reported that only versions of STIM1 that express at the ER and the PM can support ARC channel activation, thus concluding that PM-STIM1 is required for ARC channel activation by exogenous AA in HEK293 cells (Mignen et al., 2007); these results were confirmed in the present study (see section above). However, our group previously reported using an "erase and replace" strategy with STIM1 mutants and Fura2 Ca^{2+} imaging that versions of STIM1 that do not traffic to the PM and are exclusively located in the ER (ER-STIM1) are necessary and sufficient for LRC current activation by the agonist thrombin in VSMCs (Zhang et al., 2013). In light of the results described above suggesting that AA and LTC_4 likely activate the same channels in HEK293 cells and VSMCs, we reasoned that the discrepancy regarding the requirement of PM-STIM1 versus ER-STIM1 might not be caused by the cell type considered, but rather by the type of approach used in different studies. In other words, uses of Fura2 imaging on intact cells (Zhang et al., 2013) versus whole-cell patch-clamp electrophysiology where the cytosol is dialyzed with a pipette solution (Mignen et al., 2007). Therefore, we sought to perform erase and replace experiments in VSMCs similar to those described above, but instead of conducting whole-cell patch-clamp recordings, we used the less disruptive nystatin perforated patch-clamp technique. The use of the perforated patch-clamp technique prevented us from conducting recordings with LTC_4, which requires dialysis into cells. Therefore, we used this approach to measure currents activated by exogenous application of AA. Under perforated patch-clamp conditions, STIM1 knockdown efficiently abolished AA-activated currents compared with siControl cells (Fig. 7, A and B). Significantly, we could clearly determine that both WT-STIM1 (Fig. 7 C) and eYFP-STIM1 (Fig. 7 D) were capable of rescuing AA-activated currents in these STIM1-depleted VSMCs. Representative I-V curves were taken from the traces as indicated by the color-coded asterisks and are shown in Fig. 7 E, whereas statistical analyses on the extent of Na^+ currents are shown in Fig. 7 F. The differences observed between whole-cell and perforated patch-clamp results prompted us to consider that an unknown soluble factor is involved in Orai1/3 channel activation by LTC_4. Such factor might be lost under whole-cell patch-clamp recordings and thus both ER-STIM1 and PM-STIM1 would be required to support channel activation (Fig. 8 A). However, when intact cells are considered (under either Fura2 imaging or perforated patch-clamp conditions), the unknown factor is not dialyzed out and the requirement for PM-STIM1 is bypassed (Fig. 8 B). We therefore performed additional experiments to test whether the ubiquitous Ca^{2+}-binding regulatory protein calmodulin might account for this soluble factor. Pharmacological inhibition of calmodulin by calmadozolium or dialysis of calmodulin through the patch pipette failed to either inhibit or enhance LRC channel activity in response to AA (Fig. S13); note that the inclusion of calmadozolium in the bath solution affected the

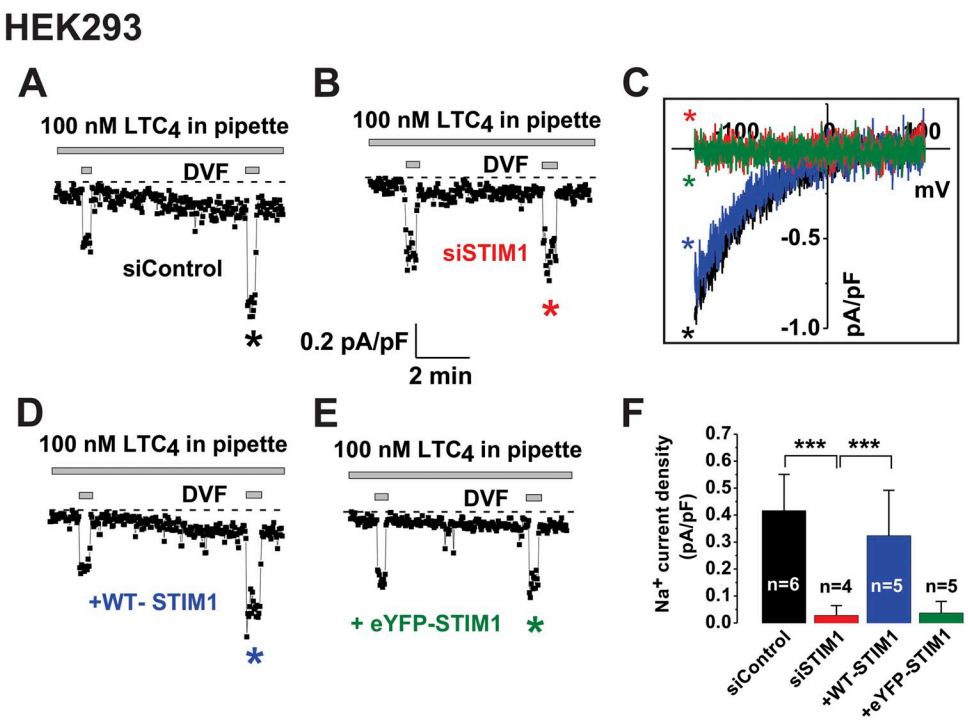

Figure 6. WT-STIM1 is required for LTC_4-activated currents in HEK293 cells. Whole-cell patch-clamp recordings in HEK293 cells transfected with siRNA against STIM1 (siSTIM1) or siControl, a nontargeting siRNA control. STIM1 knockdown abrogated LTC_4-activated Na^+/Ca^{2+} currents (B) as compared with control (A). Upon ectopic expression of plasmids encoding either WT-STIM1 (D) or eYFP-STIM1 (E) after STIM1 knockdown in HEK293 cells, only WT-STIM1 rescued LTC_4-activated currents (D and E). Representative I-V curves were taken where indicated by the color-coded asterisks and are shown in C. Statistical analysis on densities of LTC_4-activated currents for all four conditions in HEK293 cells is shown in F as mean/range.

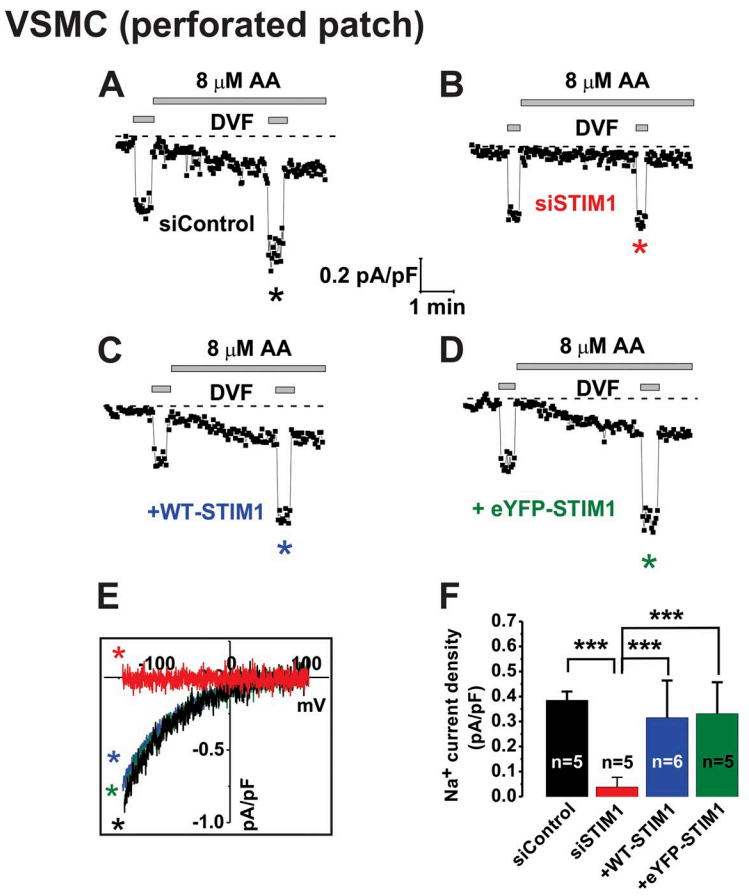

Figure 7. Under nystatin perforated patch-clamp recordings, both WT-STIM1 and eYFP-STIM1 rescued AA-activated currents. Nystatin perforated patch-clamp recordings were performed in VSMCs with 200 μg/ml nystatin in the patch pipette solution. VSMCs were transfected with siRNA against STIM1 (siSTIM1) or siControl, a nontargeting control. STIM1 knockdown completely abrogated AA-activated Na^+/Ca^{2+} currents (B) as compared with control (A). Upon ectopic expression of plasmids encoding either WT-STIM1 (C) or eYFP-STIM1 (D) after STIM1 knockdown in VSMCs, both WT-STIM1 and eYFP-STIM1 expression rescued AA-activated currents (C and D). Representative I-V curves were taken from traces where indicated by the color-coded asterisks and are shown in E. Statistical analysis on current densities for all four conditions in HEK293 cells is shown in F as mean/range.

stability of the GΩ seal and led to noisy recordings (Fig. S13 C). Importantly, we performed whole-cell patch-clamp recordings under the erase and replace conditions described above, but this time calmodulin was added to the patch pipette (Fig. S14). Calmodulin failed to support LRC currents when eYFP-STIM1 was

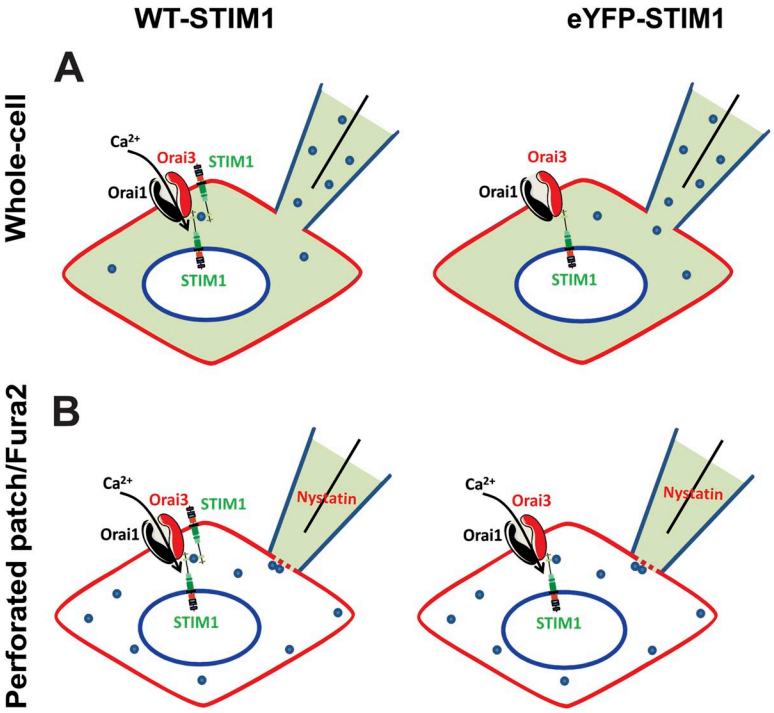

Figure 8. Hypothetical model for the requirement of PM-STIM1 and ER-STIM1 in the activation of store-independent Orai1/3 channels. This hypothetical model stipulates that an unknown cytosolic factor(s)/molecule(s) is involved in the activation by LTC_4 of a channel that is contributed by Orai1 and Orai3, which was suggested to be a pentameric assembly of three Orai1 and two Orai3 subunits (Mignen et al., 2009). Such a factor(s) might act by forming a signaling complex with STIM1 and Orai1/3. Under the whole-cell configuration (A), this unknown cytosolic factor (blue dots) is dialyzed out from the cytosol through the patch pipette (right image) unless PM-STIM1 is present to support channel activity (left image), perhaps through binding to STIM1 in the ER through STIM1/STIM1 C-terminal trans-interactions. However, when less disruptive conditions are considered (B; under either Fura2 imaging or perforated patch-clamp conditions), the unknown factor is not dialyzed out and the requirement for PM-STIM1 is bypassed (right image).

used to rescue STIM1 expression, whereas subsequent addition of ionomycin to the bath solution led to CRAC current activation (Fig. S14 C).

DISCUSSION

AA-activated Ca^{2+} signals and PM conductances were reported well before the discovery of STIM and Orai proteins as important players in Ca^{2+} signaling (Shuttleworth, 1996; Mignen and Shuttleworth, 2000). AA-activated Ca^{2+} entry or membrane currents were recorded in several cell types, including HeLa cells, RBL-1 cells, COS cells, DT40 cells, exocrine avian nasal gland cells, and mouse parotid and pancreatic acinar cells (Shuttleworth et al., 2004). However, the majority of studies characterizing ARC channels, their pharmacology, store independence, molecular correlates, and mechanisms of regulation were performed by the Shuttleworth laboratory on HEK293 cells stably transfected with the human m3 muscarinic receptor (m3-HEK293 cells) (Mignen and Shuttleworth, 2000, 2001; Mignen et al., 2003). This group showed using siRNA knockdown and overexpression that in HEK293 cells, ARC channels are encoded by both Orai1 and Orai3 (Mignen et al., 2008). Using concatenated oligomers of Orai1 and Orai3, they suggested that ARC channels are encoded by a pentamer containing three Orai1 and two Orai3 subunits (Mignen et al., 2009). Using expression of various concatenated constructs in HEK293 cells, Shuttleworth and coworkers showed that heteropentamers containing only one Orai3 subunit are sensitive to AA. However, to achieve specific selectivity for activation by AA, the heteropentamer must include two Orai3 subunits (Thompson et al., 2010). Using a chimeric approach, they further proposed that the cytosolic N-terminal domain of Orai3 is the region specifically responsible for this selectivity of activation by AA (Thompson et al., 2010). They concluded that the regulation of ARC channels by STIM1 depends exclusively on the minor pool of STIM1 residing in the PM (Mignen et al., 2007) based on patch-clamp recordings performed under two different conditions, which showed inhibition of ARC channels without significant effects on CRAC channels. These conditions are: (a) the use of a STIM1 construct in which two N-linked glycosylation sites believed essential for cell surface expression of STIM1 (Williams et al., 2002) were mutated, and (b) the treatment of intact cells with an antibody against the extracellular N-terminal domain of STIM1. In more recent work, Shuttleworth and coworkers used whole-cell patch-clamp electrophysiology to show that attachment of the cytosolic portion of STIM1 to the inner face of the PM using an N-terminal Lck domain sequence is sufficient to support AA-activated currents, while failing to support CRAC currents, suggesting that the N-terminal domain of STIM1 containing the EF-hand domain has no role in ARC channel activation (Thompson and Shuttleworth, 2012). Subsequently, using the same PM-targeted C-terminal STIM1 construct, they showed that the same region of the STIM1 C terminus that is required for CRAC channel activation (SOAR/CAD domain) is also required for ARC channel activation through constitutive association between this PM-targeted STIM1 C-terminal domain and ARC channels (Thompson and Shuttleworth, 2013).

Our laboratory is interested in primary cells of the vascular wall and their receptor-signaling mechanisms as they pertain to vascular function and disease. While screening VSMC agonists with established roles in vascular physiology and pathophysiology using Fura2 imaging and CRAC inhibitors, we identified a native Ca^{2+} entry pathway in primary VSMCs activated by the agonist thrombin that, unlike CRAC channels, was not blocked by the nonspecific inhibitor 2-APB. Nonbiased siRNA knockdown targeting all isoforms of STIM, Orai, and transient receptor potential canonical isoforms expressed in VSMCs revealed that this thrombin-activated Ca^{2+} entry pathway required STIM1, Orai1, and Orai3 (González-Cobos et al., 2013). Whole-cell patch-clamp recordings showed that this pathway is mediated by a highly Ca^{2+}-selective conductance consistent with the properties of Orai channels, but unexpectedly, we found that Ca^{2+} store depletion was not required for activation of this channel by thrombin (González-Cobos et al., 2013). Instead, cytosolic LTC_4-produced downstream thrombin receptor stimulation through the sequential catalytic activities of PLC, diacylglycerol lipase, 5-LO, and LTC_4S was the signal required for this channel activation, which we called LRC for LTC_4-regulated Ca^{2+} channel (González-Cobos et al., 2013; Zhang et al., 2013). LRC channel activation was recapitulated in whole-cell patch-clamp recordings where LTC_4 was included in the patch pipette but not when LTC_4 was applied to the bath solution (González-Cobos et al., 2013). The striking similarity between LRC channels in VSMCs and ARC channels in HEK293 cells prompted us to determine whether PM STIM1 was also required for LRC channel activation in VSMCs. However, the use of an erase and replace strategy where endogenous STIM1 was down-regulated with siRNA and then replaced with siRNA-resistant constructs reported not to traffic to the PM (eYFP-tagged STIM1 and N-linked glycosylation mutant of STIM1; Williams et al., 2002; Mercer et al., 2006) showed that these forms of STIM1 could support thrombin-activated Ca^{2+} entry measured using Fura2, suggesting that ER-resident STIM1 is required and sufficient for LRC channel activation (Zhang et al., 2013). We further showed constitutive interactions between ER-STIM1 and PM Orai3 or Orai3/Orai1 tandems (but not with Orai1) at room temperature in both VSMCs and HEK293 cells that were required for LRC channel activation by thrombin (Zhang et al., 2013). These interactions were mediated by the second C-terminal coiled-coil domain of STIM1 located within the SOAR/CAD domain (Zhang et al., 2013).

Therefore, two major differences are noted between the ARC conductance in HEK293 cells and the LRC conductance in VSMCs: (1) unlike LRC activation in VSMCs, ARC activation by AA in HEK293 cells was proposed to be independent of AA downstream metabolism; and (2) although PM-STIM1 is required for ARC channel activation in HEK293 cells, ER-STIM1 was sufficient to support LRC channel activation by agonist under Fura2 imaging conditions. To address whether these differences reflect two distinct conductances that are specific to each cell type or whether they are mediated by the same channel entity, in the present study we undertook a side by side comparison of AA- and LTC_4-activated currents in VSMCs and HEK293 cells. We showed that AA-activated currents in HEK293 cells required Orai1 and Orai3, thus confirming earlier work by Shuttleworth and colleagues (Mignen et al., 2008). We provide evidence in VSMCs and HEK293 cells that exogenously applied AA needs to be metabolized into LTC_4 to cause optimal channel activation. Prevention of AA metabolism with a 5-LO inhibitor or the application of a nonmetabolizable form of AA leads to the activation of a current that is ~50% the density of currents activated by LTC_4 dialysis through the patch pipette. Further, dialysis of a nonmetabolizable LTC_4 through the patch pipette activated currents with similar size to those activated by LTC_4, suggesting that LTC_4 is the signal required for channel activation.

We also showed that knockdown of STIM1 abrogated AA-activated currents in VSMCs and HEK293 cells, in agreement with earlier studies (Mignen et al., 2007; González-Cobos et al., 2013; Zhang et al., 2013). Significantly, when using whole-cell patch-clamp electrophysiology combined with the erase and replace approach described in Materials and methods, only nontagged WT STIM1 capable of expressing at both the ER and PM was capable of rescuing AA-activated currents in both VSMCs and HEK293 cells, in agreement with earlier studies (Mignen et al., 2007). However, when using less intrusive conditions such as the nystatin perforated patch-clamp conditions reported herein or when using intact cells, as was the case for the Fura2 imaging studies reported previously (Zhang et al., 2013), STIM1 constructs that exclusively express at the ER (ER-STIM1) were fully capable of supporting AA-activated currents. These data suggest complex roles for both ER-STIM1 and PM-STIM1 in the activation of store-independent Orai1/3 channels where ER-STIM1 is required while PM-STIM1 is likely playing a facilitatory role under physiological conditions. The cartoon in Fig. 8 depicts a hypothetical model whereby an unknown soluble factor is involved in Orai1/3 channel activation by LTC_4, which might be part of a signaling complex containing STIM1 and Orai1/3. Under whole-cell patch-clamp recordings where the cytosol is replaced with a pipette solution, PM-STIM1 is required to maintain this interaction, perhaps involving STIM1/STIM1 C-terminal trans-interactions at the ER–PM junctions where store-independent Orai1/3 channels might be located (Fig. 8 A). However, when intact cells are considered (under either Fura2 imaging or perforated patch-clamp conditions), the unknown factor is not dialyzed out and the requirement for PM-STIM1 is bypassed (Fig. 8 B). Unlike CRAC currents, which could be amplified severalfold in rescue experiments (see Figs. S10 and S12), the lack of AA- and LTC_4-activated current amplification during the rescue experiments depicted in Figs. 6 and 7 suggests that LRC currents depend on Orai3 and/or other additional cellular factors that are likely limiting in ectopic expression. We considered calmodulin as a potential candidate for this mysterious cytosolic factor required for LRC channel activation. However, pharmacological inhibition of calmodulin or dialysis of calmodulin through the patch pipette did not affect current activation by AA. Furthermore, calmodulin dialysis into the cytosol failed to rescue whole-cell currents under erase and replace when eYFP-STIM1 is used to rescue STIM1 expression. Future experiments thoroughly screening for molecular candidates are needed to test the model in Fig. 8. Such experiments will likely reveal additional players involved in the activation of store-independent Orai1/3 channel complex by LTC_4.

The authors wish to thank Dr. Bob Dirksen (University of Rochester) for suggesting the LRC (lark) channel nomenclature.

This work was mainly supported by grant R01HL097111 from the National Institutes of Health (NIH) to M. Trebak, and in part by American Heart Association grant 14GRNT18880008 to M. Trebak, grant R01HL095566 from the NIH to K. Matrougui, and Austrian Science Fund (FWF) grant M1506-B21 to I. Jardin.

The authors declare no competing financial interests.

Angus C. Nairn served as editor.

Submitted: 12 August 2013
Accepted: 29 January 2014

REFERENCES

Abdullaev, I.F., J.M. Bisaillon, M. Potier, J.C. Gonzalez, R.K. Motiani, and M. Trebak. 2008. Stim1 and Orai1 mediate CRAC currents and store-operated calcium entry important for endothelial cell proliferation. *Circ. Res.* 103:1289–1299. http://dx.doi.org/10.1161/01.RES.0000338496.95579.56

Berridge, M.J. 1993. Inositol trisphosphate and calcium signalling. *Nature.* 361:315–325. http://dx.doi.org/10.1038/361315a0

Cahalan, M.D., and K.G. Chandy. 2009. The functional network of ion channels in T lymphocytes. *Immunol. Rev.* 231:59–87. http://dx.doi.org/10.1111/j.1600-065X.2009.00816.x

Cahalan, M.D., S.L. Zhang, A.V. Yeromin, K. Ohlsen, J. Roos, and K.A. Stauderman. 2007. Molecular basis of the CRAC channel. *Cell Calcium.* 42:133–144. http://dx.doi.org/10.1016/j.ceca.2007.03.002

Clapham, D.E. 2007. Calcium signaling. *Cell.* 131:1047–1058. http://dx.doi.org/10.1016/j.cell.2007.11.028

Courjaret, R., and K. Machaca. 2012. STIM and Orai in cellular proliferation and division. *Front Biosci (Elite Ed).* E4:331–341. http://dx.doi.org/10.2741/E380

Derler, I., R. Schindl, R. Fritsch, and C. Romanin. 2012. Gating and permeation of Orai channels. *Front Biosci (Landmark Ed).* 17:1304–1322. http://dx.doi.org/10.2741/3988

Feske, S., Y. Gwack, M. Prakriya, S. Srikanth, S.H. Puppel, B. Tanasa, P.G. Hogan, R.S. Lewis, M. Daly, and A. Rao. 2006. A mutation in Orai1 causes immune deficiency by abrogating CRAC channel function. *Nature.* 441:179–185. http://dx.doi.org/10.1038/nature04702

Feske, S., E.Y. Skolnik, and M. Prakriya. 2012. Ion channels and transporters in lymphocyte function and immunity. *Nat. Rev. Immunol.* 12:532–547. http://dx.doi.org/10.1038/nri3233

González-Cobos, J.C., X. Zhang, W. Zhang, B.C. Ruhle, R.K. Motiani, R. Schindl, M. Muik, A.M. Spinelli, J.M. Bisaillon, A.V. Shinde, et al. 2013. Store-independent Orai1/3 channels activated by intracrine leukotriene C4: Role in neointimal hyperplasia. *Circ. Res.* 112:1013–1025. http://dx.doi.org/10.1161/CIRCRESAHA.111.300220

Hauser, C.T., and R.Y. Tsien. 2007. A hexahistidine-Zn^{2+}-dye label reveals STIM1 surface exposure. *Proc. Natl. Acad. Sci. USA.* 104:3693–3697. http://dx.doi.org/10.1073/pnas.0611713104

Hogan, P.G., and A. Rao. 2007. Dissecting ICRAC, a store-operated calcium current. *Trends Biochem. Sci.* 32:235–245. http://dx.doi.org/10.1016/j.tibs.2007.03.009

Hogan, P.G., R.S. Lewis, and A. Rao. 2010. Molecular basis of calcium signaling in lymphocytes: STIM and ORAI. *Annu. Rev. Immunol.* 28:491–533. http://dx.doi.org/10.1146/annurev.immunol.021908.132550

Hoth, M., and R. Penner. 1992. Depletion of intracellular calcium stores activates a calcium current in mast cells. *Nature.* 355:353–356. http://dx.doi.org/10.1038/355353a0

Lewis, R.S. 2011. Store-operated calcium channels: New perspectives on mechanism and function. *Cold Spring Harb. Perspect. Biol.* 3:a003970. http://dx.doi.org/10.1101/cshperspect.a003970

Liou, J., M.L. Kim, W.D. Heo, J.T. Jones, J.W. Myers, J.E. Ferrell Jr., and T. Meyer. 2005. STIM is a Ca^{2+} sensor essential for Ca^{2+}-store-depletion-triggered Ca^{2+} influx. *Curr. Biol.* 15:1235–1241. http://dx.doi.org/10.1016/j.cub.2005.05.055

Lompre, A.M., L. Benard, Y. Saliba, F. Aubart, J. Fauconnier, and J.S. Hulot. 2013. STIM1 and Orai in cardiac hypertrophy and vascular proliferative diseases. *Front Biosci (Schol Ed).* S5:766–773. http://dx.doi.org/10.2741/S406

Mercer, J.C., W.I. Dehaven, J.T. Smyth, B. Wedel, R.R. Boyles, G.S. Bird, and J.W. Putney Jr. 2006. Large store-operated calcium selective currents due to co-expression of Orai1 or Orai2 with the intracellular calcium sensor, Stim1. *J. Biol. Chem.* 281:24979–24990. http://dx.doi.org/10.1074/jbc.M604589200

Mignen, O., and T.J. Shuttleworth. 2000. I_{ARC}, a novel arachidonate-regulated, noncapacitative Ca^{2+} entry channel. *J. Biol. Chem.* 275:9114–9119. http://dx.doi.org/10.1074/jbc.275.13.9114

Mignen, O., and T.J. Shuttleworth. 2001. Permeation of monovalent cations through the non-capacitative arachidonate-regulated Ca^{2+} channels in HEK293 cells. Comparison with endogenous store-operated channels. *J. Biol. Chem.* 276:21365–21374. http://dx.doi.org/10.1074/jbc.M102311200

Mignen, O., J.L. Thompson, and T.J. Shuttleworth. 2003. Ca^{2+} selectivity and fatty acid specificity of the noncapacitative, arachidonate-regulated Ca^{2+} (ARC) channels. *J. Biol. Chem.* 278:10174–10181. http://dx.doi.org/10.1074/jbc.M212536200

Mignen, O., J.L. Thompson, and T.J. Shuttleworth. 2007. STIM1 regulates Ca^{2+} entry via arachidonate-regulated Ca^{2+}-selective (ARC) channels without store depletion or translocation to the plasma membrane. *J. Physiol.* 579:703–715. http://dx.doi.org/10.1113/jphysiol.2006.122432

Mignen, O., J.L. Thompson, and T.J. Shuttleworth. 2008. Both Orai1 and Orai3 are essential components of the arachidonate-regulated Ca^{2+}-selective (ARC) channels. *J. Physiol.* 586:185–195. http://dx.doi.org/10.1113/jphysiol.2007.146258

Mignen, O., J.L. Thompson, and T.J. Shuttleworth. 2009. The molecular architecture of the arachidonate-regulated Ca^{2+}-selective ARC channel is a pentameric assembly of Orai1 and Orai3 subunits. *J. Physiol.* 587:4181–4197. http://dx.doi.org/10.1113/jphysiol.2009.174193

Motiani, R.K., X. Zhang, K.E. Harmon, R.S. Keller, K. Matrougui, J.A. Bennett, and M. Trebak. 2013. Orai3 is an estrogen receptor α-regulated Ca^{2+} channel that promotes tumorigenesis. *FASEB J.* 27:63–75. http://dx.doi.org/10.1096/fj.12-213801

Park, C.Y., P.J. Hoover, F.M. Mullins, P. Bachhawat, E.D. Covington, S. Raunser, T. Walz, K.C. Garcia, R.E. Dolmetsch, and R.S. Lewis. 2009. STIM1 clusters and activates CRAC channels via direct binding of a cytosolic domain to Orai1. *Cell.* 136:876–890. http://dx.doi.org/10.1016/j.cell.2009.02.014

Prakriya, M. 2013. Store-operated Orai channels: Structure and function. *Curr Top Membr.* 71:1–32. http://dx.doi.org/10.1016/B978-0-12-407870-3.00001-9

Prakriya, M., and R.S. Lewis. 2002. Separation and characterization of currents through store-operated CRAC channels and Mg^{2+}-inhibited cation (MIC) channels. *J. Gen. Physiol.* 119:487–508. http://dx.doi.org/10.1085/jgp.20028551

Putney, J.W., Jr. 1990. Capacitative calcium entry revisited. *Cell Calcium.* 11:611–624. http://dx.doi.org/10.1016/0143-4160(90)90016-N

Roos, J., P.J. DiGregorio, A.V. Yeromin, K. Ohlsen, M. Lioudyno, S. Zhang, O. Safrina, J.A. Kozak, S.L. Wagner, M.D. Cahalan, et al. 2005. STIM1, an essential and conserved component of store-operated Ca^{2+} channel function. *J. Cell Biol.* 169:435–445. http://dx.doi.org/10.1083/jcb.200502019

Shinde, A.V., R.K. Motiani, X. Zhang, I.F. Abdullaev, A.P. Adam, J.C. González-Cobos, W. Zhang, K. Matrougui, P.A. Vincent, and M. Trebak. 2013. STIM1 controls endothelial barrier function independently of Orai1 and Ca^{2+} entry. *Sci. Signal.* 6:ra18. http://dx.doi.org/10.1126/scisignal.2003425

Shuttleworth, T.J. 1996. Arachidonic acid activates the noncapacitative entry of Ca^{2+} during $[Ca^{2+}]_i$ oscillations. *J. Biol. Chem.* 271:21720–21725.

Shuttleworth, T.J. 2012. STIM and Orai proteins and the non-capacitative ARC channels. *Front Biosci (Landmark Ed).* 17:847–860. http://dx.doi.org/10.2741/3960

Shuttleworth, T.J., J.L. Thompson, and O. Mignen. 2004. ARC channels: A novel pathway for receptor-activated calcium entry. *Physiology (Bethesda).* 19:355–361. http://dx.doi.org/10.1152/physiol.00018.2004

Srikanth, S., and Y. Gwack. 2012. Orai1, STIM1, and their associating partners. *J. Physiol.* 590:4169–4177. http://dx.doi.org/10.1113/jphysiol.2012.231522

Srikanth, S., and Y. Gwack. 2013. Orai1-NFAT signalling pathway triggered by T cell receptor stimulation. *Mol. Cells.* 35:182–194. http://dx.doi.org/10.1007/s10059-013-0073-2

Thompson, J.L., and T.J. Shuttleworth. 2012. A plasma membrane-targeted cytosolic domain of STIM1 selectively activates ARC channels, an arachidonate-regulated store-independent Orai channel. *Channels (Austin).* 6:370–378. http://dx.doi.org/10.4161/chan.21947

Thompson, J.L., and T.J. Shuttleworth. 2013. Molecular basis of activation of the arachidonate-regulated Ca^{2+} (ARC) channel, a store-independent Orai channel, by plasma membrane STIM1. *J. Physiol.* 591:3507–3523.

Thompson, J., O. Mignen, and T.J. Shuttleworth. 2010. The N-terminal domain of Orai3 determines selectivity for activation of the store-independent ARC channel by arachidonic acid. *Channels (Austin).* 4:398–410. http://dx.doi.org/10.4161/chan.4.5.13226

Trebak, M. 2012. STIM/Orai signalling complexes in vascular smooth muscle. *J. Physiol.* 590:4201–4208. http://dx.doi.org/10.1113/jphysiol.2012.233353

Vig, M., C. Peinelt, A. Beck, D.L. Koomoa, D. Rabah, M. Koblan-Huberson, S. Kraft, H. Turner, A. Fleig, R. Penner, and J.P. Kinet. 2006. CRACM1 is a plasma membrane protein essential for store-operated Ca^{2+} entry. *Science*. 312:1220–1223. http://dx.doi.org/10.1126/science.1127883

Williams, R.T., P.V. Senior, L. Van Stekelenburg, J.E. Layton, P.J. Smith, and M.A. Dziadek. 2002. Stromal interaction molecule 1 (STIM1), a transmembrane protein with growth suppressor activity, contains an extracellular SAM domain modified by N-linked glycosylation. *Biochim. Biophys. Acta*. 1596:131–137. http://dx.doi.org/10.1016/S0167-4838(02)00211-X

Yuan, J.P., W. Zeng, M.R. Dorwart, Y.J. Choi, P.F. Worley, and S. Muallem. 2009. SOAR and the polybasic STIM1 domains gate and regulate Orai channels. *Nat. Cell Biol.* 11:337–343. http://dx.doi.org/10.1038/ncb1842

Zhang, S.L., A.V. Yeromin, X.H. Zhang, Y. Yu, O. Safrina, A. Penna, J. Roos, K.A. Stauderman, and M.D. Cahalan. 2006. Genome-wide RNAi screen of Ca^{2+} influx identifies genes that regulate Ca^{2+} release-activated Ca^{2+} channel activity. *Proc. Natl. Acad. Sci. USA*. 103:9357–9362. http://dx.doi.org/10.1073/pnas.0603161103

Zhang, W., K.E. Halligan, X. Zhang, J.M. Bisaillon, J.C. Gonzalez-Cobos, R.K. Motiani, G. Hu, P.A. Vincent, J. Zhou, M. Barroso, et al. 2011. Orai1-mediated I (CRAC) is essential for neointima formation after vascular injury. *Circ. Res.* 109:534–542. http://dx.doi.org/10.1161/CIRCRESAHA.111.246777

Zhang, X., J.C. González-Cobos, R. Schindl, M. Muik, B. Ruhle, R.K. Motiani, J.M. Bisaillon, W. Zhang, M. Fahrner, M. Barroso, et al. 2013. Mechanisms of STIM1 activation of store-independent leukotriene C4-regulated Ca^{2+} channels. *Mol. Cell. Biol.* 33:3715–3723. http://dx.doi.org/10.1128/MCB.00554-13